

## Research Article

# Enhancement Modelling Based on Electrical Discharge Machining Successive Discharges

**Farook Nehad Abed** <sup>1</sup>, **V. Ramesh** <sup>2</sup>, **Mohanad Fadhil Jwaid**,<sup>3</sup> **Nidhi Agarwal**,<sup>4</sup> **Deepika Koundal**,<sup>5</sup> and **Abdelrahman Mohamed Ibrahim** <sup>6</sup>

<sup>1</sup>Faculty of Mechanical, Manufacturing Engineering, Imam Al-Adham University College, Baghdad, Iraq

<sup>2</sup>Research Department of Mathematics, Kandaswami Kandari's College, Velur, Namakkal, Tamilnadu, India

<sup>3</sup>Al-Imam University College, Riyadh, Saudi Arabia

<sup>4</sup>Department of Information Technology, KIET Group of Institutions, Delhi-NCR, Ghaziabad, India

<sup>5</sup>Department of Systemics, University of Petroleum & Energy Studies, Dehradun, India

<sup>6</sup>Accounting and Financial Management School of Management Studies, University of Khartoum, Khartoum, Sudan

Correspondence should be addressed to Abdelrahman Mohamed Ibrahim; [amibrahim@uofk.edu](mailto:amibrahim@uofk.edu)

Received 11 December 2021; Revised 28 December 2021; Accepted 4 January 2022; Published 15 January 2022

Academic Editor: Palanivel Velmurugan

Copyright © 2022 Farook Nehad Abed et al. This is an open access article distributed under the Creative Commons Attribution License, which permits unrestricted use, distribution, and reproduction in any medium, provided the original work is properly cited.

The surface roughness of Inconel 718 is predicted using a sequential discharge model for electrical discharge machining (EDM). To begin with, the EDM single pulse discharge machining process was accurately simulated using the finite-element method (FEM). The surface topography under various discharge settings, the size, and the characteristic parameters of a single-pulse crater are simulated. Second, the material defines the discharge position as the minimum gap width between the work piece's starting surface and the electrode in the removal model. The simulation shows that the magnitude of the single-pulse discharge energy influences the crater's form and size. A difference in discharge energy causes a divergence in the increasing crater radius, depth, and flanging height trends. On the other hand, the ultimate surface morphology of an EDM machined surface is determined by the distribution of discharge locations around the parts in the workpiece; finally, machined surfaces are inspected using the same discharge parameters. The EDM work piece's surface morphology matches the material removal. Between simulation and experiment, there is a relative error in surface roughness around 8.26%, and there is a relative error in surface roughness.

## 1. Introduction

EDM uses the instantaneous local high temperature generated by the pulse. Cast iron material has the characteristics of spark discharge between the workpiece and the high strength, wear resistance, and heat resistance. Electrode wire to melt and vaporize in all cast iron materials uses Inconel 718 (grey cast workpiece material, to achieve the purpose of iron) because of its corrosion resistance and shock removal. Compared with the absorption and excellent casting performance of traditional machining, EDM makes use of other characteristics often used in the electrode wire to keep a certain distance from the manufacture of machine tool bed and column workpiece, and it can achieve high-precision machining [1].

When machining cast iron materials by EDM, not only the surface deformation of the workpiece is small but also there is almost no environmental pollution in the whole machining process. These characteristics make EDM suitable for machining Inconel 718 materials [2]. However, due to the randomness and disorder in the EDM process, the surface roughness of processed materials often cannot reach the predetermined standard, and instruments and equipment cannot directly observe the processing of materials in the process of machining, so the surface roughness of processed materials cannot be accurately controlled. In the EDM process, discharge parameters play an important role in surface roughness, and many researchers control surface roughness by optimizing discharge parameters [3, 4]. The Taguchi

method is commonly used to improve the EDM process, and the best parameters can all be found through experimentation through statistical analysis. [5] conducted primary research on EDM from mechanical and electrical principles and provided fundamental insights on EDM processing. [6] studied the effects of WDEM process parameters such as the cutting radius of a workpiece, water flow, and the wire feed rate on the surface roughness of alumina particle-reinforced materials and optimized the process parameters. Chaudhary et al. [7] used the heat transfer search algorithm to conduct multiresponse optimization of process parameters for EDM machining of superelastic Ni-Ti-N shape memory alloy. At present, based on the principle of EDM, the establishment of a material removal model based on successive discharges is always considered to be a challenging job. Furthermore, there have been very few studies on the modeling of surface roughness caused by the EDM process. Various extensive mathematic models and simulation methodologies have been devised to model EDM processes. In an EDM procedure, Tao and Ni et al. [8] developed a model to mimic discharge crater formation by considering the effect of bubble pressures to obtain very good crater geometry. [3] simulated the formation of craters in EDM using the molecular dynamics method while taking into account the pressure of the medium between the electrodes. The rate of material removal is found to be faster when the medium pressure is higher. In studying final surface morphology formation, the establishment of a single-pulse discharge crater model in EDM is critical formation [9]. The EDM process, in which the workpiece surface is built by the superposition of craters formed by numerous discharges, cannot be explained by the production of a single crater [10]. [11] have carried out a numerical analysis using the finite difference method. They were able to predict the material removal rate and surface roughness with a 6 percent margin of error using inverted identification. [2, 12–19] established a surface topography prediction model under EDM continuous discharge based on FEM, and Ra simulation results were consistent with experimental results. [20–24] established a model based on 3D continuous discharge to study the relationship between workpiece surface topography and electrode wire vibration. Results: in the SV-MF composite-assisted EDM process, the surface roughness of the workpiece decreases by more than 10%, and the uniformity of the discharge position distribution is improved. Experiments back up the numerical model, and also, the simulated error for surface roughness is a little less than 5%.

A 3D material removal system is proposed in this study to simulate the removal of materials. Successive discharges machining process of EDM: the relationship between single-pulse crater morphology, discharge position, and dynamic surface morphology is established. Meanwhile, the effects of the molten vaporization of the processed material and the residual heat generated by a single spark are considered for simulation. The impact of different discharge energies in singular pulse discharge models is created by studying the

impact crater's surface form and size. Minimum gap width determines discharge position, rather than assuming a random distribution of discharge position, which is more consistent with the actual EDM machining process. Several profile lines were extracted from the 3D material removal model, and the characteristic parameters were determined through averaging to predict the surface roughness. This study used pulse width and peak current as input parameters, and surface roughness was used as the output parameter. Experiments verified the accuracy of the continuous discharge material removal model in predicting surface roughness.

## 2. Experimental Details

The continuous discharge material removal model was verified on the EDM (CHMER EDM) machine. The dielectric was emulsion, and the electrode was 20 mm. Figure 1 shows the experimental setup. The workpiece material is Inconel 718, and the dimensions of the specimens were  $10 \times 10 \times 5$  mm. The percentage of chemical composition properties of the workpiece material is given in Table 1. Pulse width ( $T_{on}$   $\mu$ s) and peak current ( $I_p$  A) were used as independent input parameters, and surface roughness ( $R_a$   $\mu$ m) was used as output parameters. The levels of the independent parameters are shown in Table 2. The other parameters, 120 V open-circuit voltage, 1 : 3 interval ratio, 4 m/min, 5 kg/cm<sup>2</sup> dielectric flushing pressure, and 9 kg wire tension, were kept constant during the experiments.

As a first step, the surface roughness of each machined material was unified by grinding, and the original surface roughness of each machined material was controlled between 1.3  $\mu$ m and 1.5  $\mu$ m. Secondly, in the normal machining process of EDM, the discharge is continuous, and the crater is superimposed on each other, so it is almost impossible to study every single-pulse discharge crater. Therefore, to conform to the assumed conditions of the material removal model as much as possible and at the same time, to obtain a single crater, another series of experiments were designed with apparent surface morphology on the continuous electric discharge machining surface. An often overlooked but important idea is to find the distance between the molybdenum wire and the workpiece at which the spark discharge occurs in the first contact. The motion distance of the molybdenum wire can be detected by using the coordinate motion system of the EDM machine (CHMER EDM) machine. The experimental steps are shown in Figure 1. Firstly, the initial gap between the continuous discharge material removal model was verified on the EDM machine (CHMER EDM). The dielectric was emulsion, and the electrode wire was 0.18 mm molybdenum wire. Figure 1 shows the experimental setup. The workpiece material is Inconel 718, and the dimensions of the specimens were  $10 \times 10 \times 5$  mm. The percentage of chemical composition properties of the workpiece material is given in Table 1. Pulse width ( $T_{on}$   $\mu$ s) and peak current ( $I_p$  A) were used as independent input parameters, and surface roughness ( $R_a$   $\mu$ m) was used as the output parameter. The levels of the independent parameters are shown in Table 3. During the



FIGURE 1: EDM machine (CHMER EDM).

TABLE 1: Chemical composition properties of Inconel 718.

| Chemical composition (%) | Ni | Fe      | C    | Al   | Ti   | Si   | Mn   | P     | S    |
|--------------------------|----|---------|------|------|------|------|------|-------|------|
|                          | 50 | Balance | 0.08 | 0.20 | 0.65 | 0.35 | 0.35 | 0.015 | 0.18 |

TABLE 2: Factors and levels for the experiment.

| No.                    | 1  | 2  | 3  | 4  | 5  | 6  | 7  | 8  | 9  |
|------------------------|----|----|----|----|----|----|----|----|----|
| Peak current (A)       | 10 | 10 | 10 | 14 | 14 | 14 | 18 | 18 | 18 |
| Pulse width ( $\mu$ s) | 14 | 14 | 14 | 26 | 26 | 26 | 34 | 34 | 34 |

TABLE 3: Comparison of surface roughness values.

| No. | Experimental Ra ( $\mu$ m) | Model Ra ( $\mu$ m) | Error (%) |
|-----|----------------------------|---------------------|-----------|
| 1   | 4.22                       | 3.78                | 5.29      |
| 2   | 4.34                       | 3.89                | 2.27      |
| 3   | 4.54                       | 3.78                | 2.35      |
| 4   | 6.33                       | 5.87                | 7.53      |
| 5   | 6.89                       | 6.22                | 7.9       |
| 6   | 9.12                       | 8.89                | 5.18      |
| 7   | 10.45                      | 9.66                | 9.77      |
| 8   | 11.76                      | 10.87               | 7.86      |
| 9   | 12.45                      | 11.34               | 15.16     |

experiments, the other parameters, 120 V open-circuit voltage, 1:3 interval ratio, 4 m/min, 5 kg/cm<sup>2</sup> dielectric flushing pressure, 9 kg wire tension, and 0.18 mm wire diameter, were kept constant.

As a first step, the surface roughness of each machined material was unified by grinding, and the original surface roughness of each machined material was controlled between 1.3  $\mu$ m and 1.5  $\mu$ m. Secondly, in the normal machining process of EDM, the discharge is continuous, and the crater is superimposed on each other, so it is almost impossible to study every single pulse discharge crater. Therefore, to conform to the assumed conditions of the material removal model as much as possible and at the same time, to obtain a single crater, another series of experiments were designed with apparent surface morphology on the

continuous electric discharge machining surface. An often overlooked but important idea is to find the distance between the molybdenum wire and the workpiece at which the spark discharge occurs in the first contact. The motion distance of the copper tool can be detected by using the coordinate motion system of the EDM machine (CHMER EDM). The experimental steps are shown in Figure 1. Firstly, the initial gap between the copper tool and the workpiece is controlled at 1 mm, and then, the discharge machining of the material surface is carried out. Finally, the discharge parameters were adjusted by the EDM operating panel. The comparative experiments of nine groups were carried out, and workpieces are controlled at 1 mm, and then, the discharge machining of the material surface is carried out. Finally, the discharge parameters were adjusted by the EDM operating panel, and the comparative experiments of nine groups were carried out.

White light scanning interferometry: To acquire the average roughness and three-dimensional shape image of the material machined surface, we installed the sample on the noncontact preview W1 optical 3D surface profiler. Images of 489.5  $\mu$ m  $\times$  489.5  $\mu$ m area were acquired accordingly. Surface composition measurement: to measure the composition of the material surface after EDM, the machined surface was sampled and measured by X-ray diffraction (XRD).

### 3. Experimental Results and Discussion

Each experimental material's final surface morphology and crater morphology were analyzed using three-dimensional morphological images. Figure 2 shows a crater's surface topography and size metrics. It is found that the radius of the

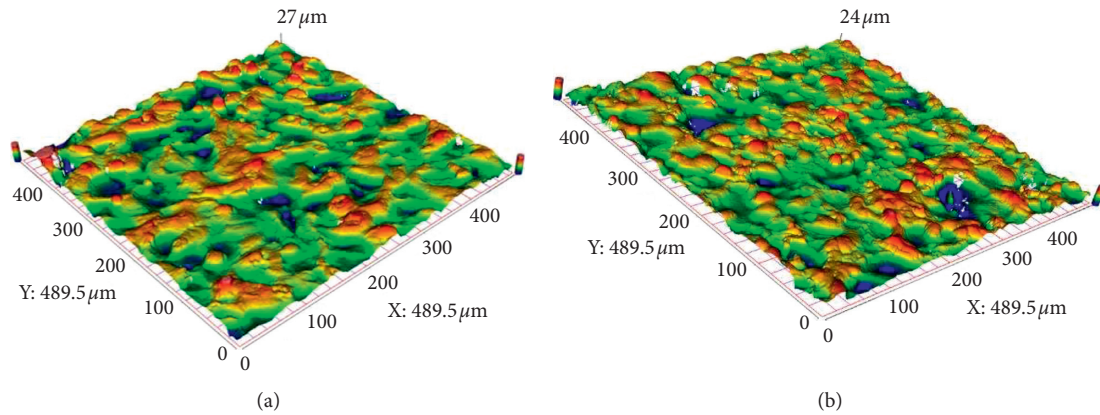


FIGURE 2: Surface topography of EDM continuous discharge: 3D view and crater shape and dimensions ( $I_p = 10$  A,  $T_{on} = 14$   $\mu$ s).

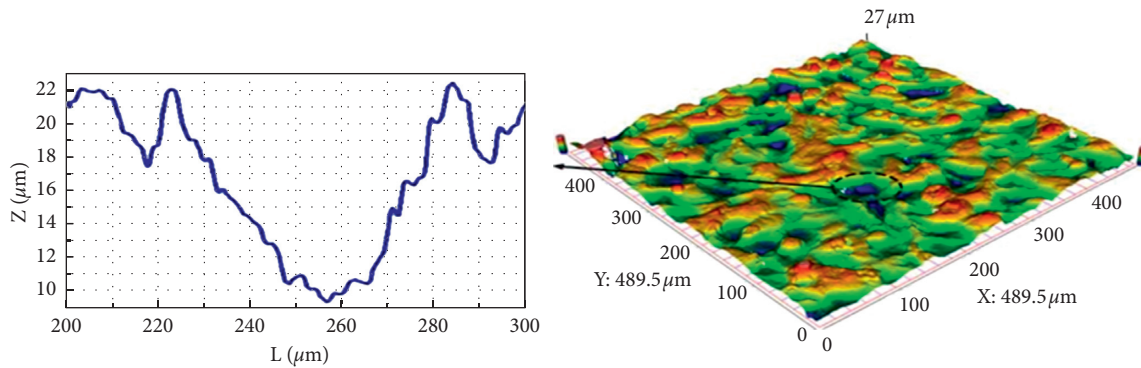


FIGURE 3: 3D micrometer surface morphology with different discharge energies: (a)  $I_p = 14$  A,  $T_{on} = 26$   $\mu$ s; (b)  $I_p = 18$  A,  $T_{on} = 34$   $\mu$ s.

crater is 50–80  $\mu$ m, the depth of the crater is 6  $\mu$ m–10  $\mu$ m, and the flanging height is 2  $\mu$ m–8  $\mu$ m. This is consistent with the characteristic parameters of the single-pulse discharge crater model obtained by the previous simulation. Figure 3 shows the machined surface topography with different discharge parameters; as the discharge energy increases as more material is taken from the workpiece, the material removed increases. The size and number of craters on the workpiece surface: at the same time, in the process of crater formation, with the rise of discharge energy, the crater size increase is not synchronized, the crater diameter increase scope is more prominent, and the growth rate is the fastest, then the indentation depth is used to achieve the stable value, and finally, because of the effect of processing waste heat of molten material flow trend, flanging height also gradually achieves the typical value. The variation trend of crater size characteristic parameters with discharge energy during simulation is verified.

After the experiment, the material's surface was observed by using a scanning electron microscope (SEM), and XRD measurements were made. The composition of the surface of the material is shown in Figure 4. The change of chemical composition and microstructure of the surface layer after EDM machining verified the phase transition of the material surface caused by heat during the simulation process of single-pulse discharge

**3.1. Model Validation.** Figure 5 depicts an example of a simulated and an experimental surface. To verify the accuracy of the predicted surface roughness of the material removal model, the measured surface roughness is compared with the expected surface roughness of the model. The surface roughness and average error between the experimental results and the simulation results are shown in Table 3 and Figure 6. The predicted values of the model are consistent with the experimental measurements. The average relative error of the EDM continuous discharge material removal model established in this paper to predict the surface roughness is 8.26%. There is a particular error between the measured value and the expected value of the model because there are many influencing factors in the experiment and modeling process. In the process of single-pulse discharge simulation, the grid division, the selection of energy distribution coefficient and convective heat transfer coefficient, and the measurement of thermal properties of Inconel 718 material at different temperatures have a particular influence on the accuracy of simulation results. In the actual machining process of EDM, the regular discharge, arc discharge, and short-circuit discharge states are inevitable. However, different types of discharge states have different discharge energy levels. This phenomenon makes the changes of each discharge crater inconsistent, increasing surface roughness.



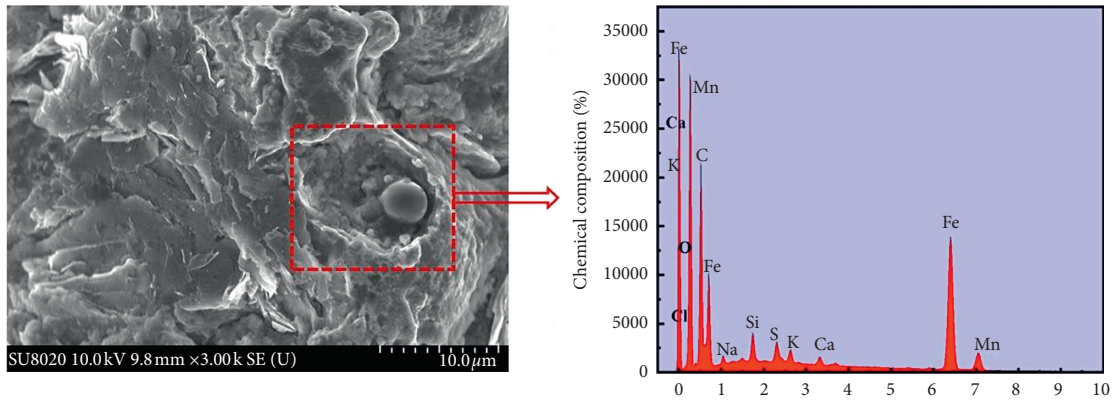


FIGURE 4: SEM micrograph and the corresponding XRD spectrum of the microcrater.

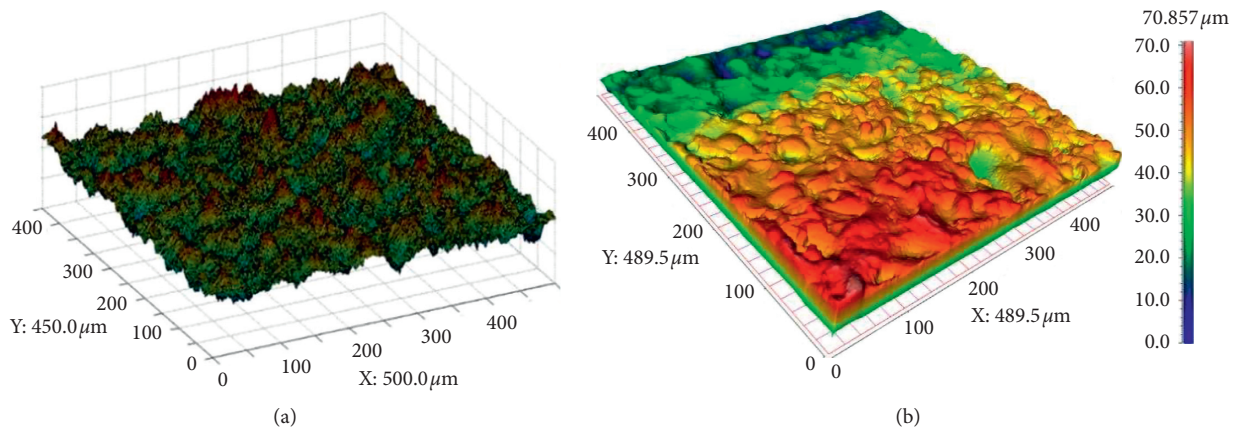


FIGURE 5: Experimental and simulated surface topographies: (a) simulated result; (b) experimental result.

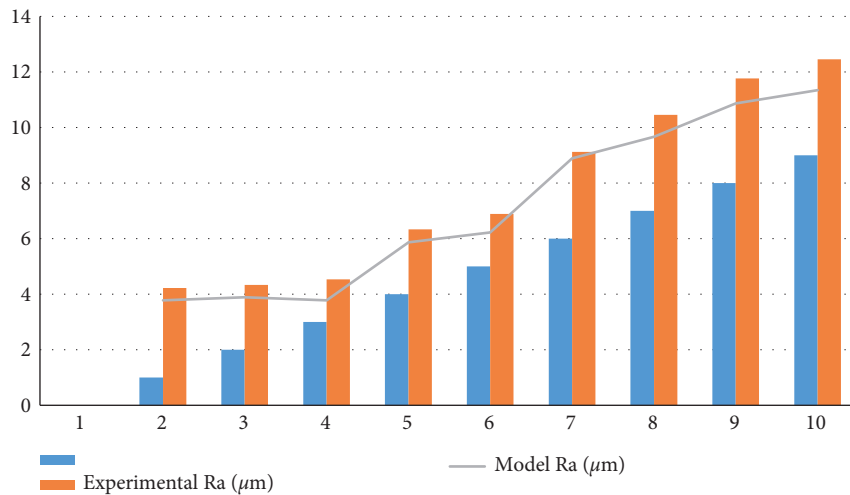


FIGURE 6: Comparison of Ra values of the simulation and experiment.

3.2. Influence of Discharge Parameters on Surface Roughness. Figure 7 shows the relationship between peak current, pulse width, and surface roughness. Surface roughness rises as peak current and pulse width increase, and the effect of peak current on surface roughness is greater than that of the pulse width. When the discharge current and the increase of pulse

width mean the addition of single-pulse discharging energy, according to the simulation result, it is shown that, in front of a single-pulse discharge energy increase, in the process of heat transfer of radial direction in the pits, the discharge rate of growth is greater than the depth direction, thus forming the discharge crater diameter growth rate greater than the

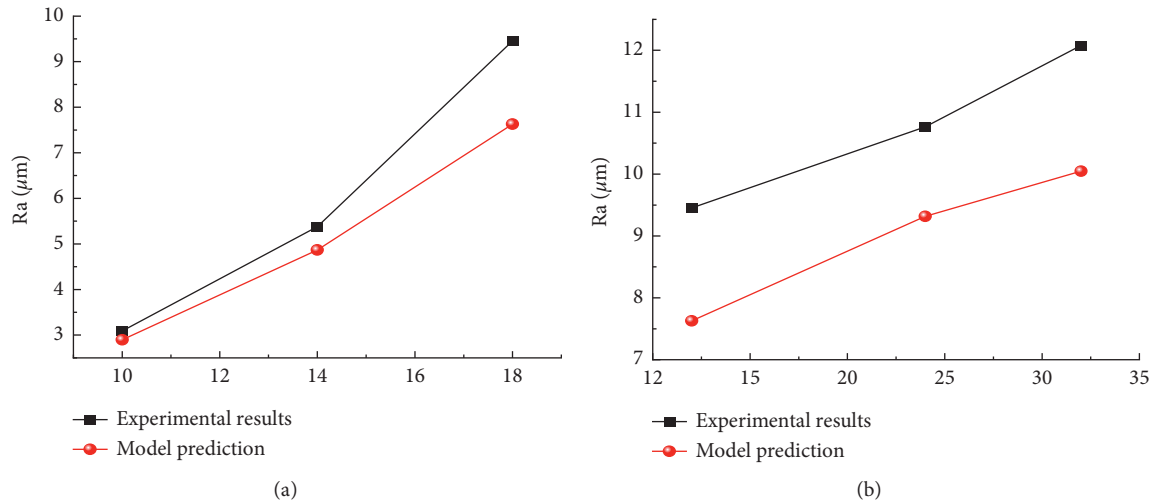


FIGURE 7: The relationship between (a) peak current and surface roughness and (b) pulse width and surface roughness. (a) Peak current (A); (b) pulse width ( $\mu\text{s}$ ).

depth of the growth rate; finally, the surface roughness increases with the increase of discharge current and pulse width.

#### 4. Conclusions

From the analysis as mentioned above and experiments, the following conclusions can be drawn.

According to the energy conservation theorem, different discharge parameters replicate the impact crater's characteristic size.

- (1) Peak current and pulse width impact discharge pit temperature and velocity. The increasing crater radius, depth, and deformation heights are not related to increased discharge energy, but to variable factors. The crater's radius changes in synchrony with the increasing trend. The material removal model uses EDM machining mechanism.
- (2) Continuous discharge was established to simulate the procedure of machining. Peak current and pulse width are used as inputs, and surface roughness is used as an output measure. The workpiece's initial surface topography and the electrode wire with a minimum gap width were taken as the discharge position. Then, the material removal model was tested by experiments. The results show that the prediction accuracy of the EDM continuous discharge material removal model for surface roughness is around 8.26%. The surface roughness increases with the increase of peak current and pulse width, and the effect of the peak current on surface roughness is greater than that of the pulse width.
- (3) It can also precisely estimate the eventual surface shape of materials following continuous discharge. Adjusting discharge parameters improves EDM machining accuracy and surface integrity. To better anticipate the material erosion surface created by

continuous pulse discharge, the influence of electric field was incorporated into the model continuous pulse discharge to achieve a more accurate prediction.

#### Data Availability

The data underlying the results presented in the study are available within the manuscript.

#### Conflicts of Interest

The authors declare that there are no conflicts of interest regarding the publication of this paper.

#### References

- [1] S. K. Gauri and S. Chakraborty, "A study on the performance of some multi-response optimisation methods for WEDM processes," *International Journal of Advanced Manufacturing Technology*, vol. 49, no. 1-4, pp. 155-166, 2010.
- [2] A. Bin Sapit, S. Kariem Shather, and F. Nehad Abed, "Enhancement of the performance surface roughness of wire cutting process by additives Nano ( $\text{Al}_2\text{O}_3$ )," *Let's Save the World and Humanity*, vol. 8, no. 2, pp. 933-941, 2020.
- [3] A. Abdullah Hamad, M. Lellis Thivagar, M. Bader Alazzam et al., "Dynamic systems enhanced by electronic circuits on 7D," *Advances in Materials Science and Engineering*, vol. 2021, Article ID 8148772, 11 pages, 2021.
- [4] V. Anand, S. Gupta, D. Koundal, S. Mahajan, and A. Kant Pandit, "Deep learning based automated diagnosis of skin diseases using dermoscopy," *CMC-Computers, Materials & Continua*, vol. 71, no. 2, pp. 3145-3160, 2022.
- [5] L. Malacrida, S. Ranjit, D. M. Jameson, and E. Gratton, "The phasor plot: a universal circle to advance fluorescence lifetime analysis and interpretation," *Annual Review of Biophysics*, vol. 50, pp. 575-593, 2021.
- [6] L. Wang, A. A. Hamad, and V. Sakthivel, "IoT assisted machine learning model for warehouse management," *Journal of Interconnection Networks*, vol. 3, Article ID 2143005, 2021.

- [7] S. Patel, D. Thesiya, and A. Rajurkar, "Aluminium powder mixed rotary electric discharge machining (PMEDM) on Inconel 718," *Australian Journal of Mechanical Engineering*, vol. 16, no. 1, pp. 21–30, 2018.
- [8] F. Nehadabed, A. Bin Sapit, and S. Kariemshather, "An analysis of wire-cut parameters IN electric-discharge of titanium alloys," 2019, <http://www.tjprc.org>.
- [9] L. W. Reolon, C. A. Henning Laurindo, R. D. Torres, and F. L. Amorim, "WEDM performance and surface integrity of Inconel alloy IN718 with coated and uncoated wires," *International Journal of Advanced Manufacturing Technology*, vol. 100, no. 5–8, pp. 1981–1991, 2019.
- [10] D. Kumar, S. Chakraborty, A. Ranjan, and D. Bose, "Experimental study on improving material removal rate and surface roughness in wire-cut EDM of low conductive material," in *Advances in Unconventional Machining and Composites*, pp. 113–126, Springer, Singapore, 2020.
- [11] S. Singh, I. Gupta, S. Gupta, D. Koundal, and S. Aljahdali, "Deep learning based automated detection of diseases from apple leaf images," *CMC-Computers, Materials & Continua*, vol. 71, no. 1, pp. 1849–1866, 2022.
- [12] S. K. Shather, A. F. Ibrahim, and N. Jammal, "Influence of EDM parameters on the appearance of recast layer," *Journal of Engineering Technology*, vol. 35, pp. 694–700, 2017.
- [13] M. Alsaffar, A. A. Hamad, A. Alshammari et al., "Network management system for IoT based on dynamic systems," *Computational and Mathematical Methods in Medicine*, vol. 2021, Article ID 9102095, 8 pages, 2021.
- [14] K. Bhalla, D. Koundal, S. Bhatia, M. K. I. Rahmani, and M. Tahir, "Fusion of infrared and visible images using fuzzy based siamese convolutional network," *CMC-Computers Materials & Continua*, vol. 70, no. 3, pp. 5503–5518, 2022.
- [15] R. A. Shah and A. Darji, "An experimental effect of soft brass wire on MRR, kerf width and surface roughness of AISI D2 tool steel in WEDM," *Materials Today Proceedings*, vol. 3, no. 5, pp. 1–3, 2018.
- [16] B. A. Ahmed, S. K. Shather, and W. K. Hamdan, "Effect of single point incremental forming parameters on spring back and micro-crack density," *AIP Conference Proceedings*, vol. 2213, 2020.
- [17] G. Alshammari, A. A. Hamad, Z. M. Abdullah et al., "Applications of deep learning on topographic images to improve the diagnosis for dynamic systems and unconstrained optimization," *Wireless Communications and Mobile Computing*, vol. 2021, Article ID 4672688, 7 pages, 2021.
- [18] B. A. Al-Rahawe, A. A. Hamad, M. H. Al-Zuhairy, H. H. Khalaf, and S. Abebaw, "The commitment of Nineveh governorate residents to the precautionary measures against global 2019 pandemic and dermatological affection of precautions," *Applied Bionics and Biomechanics*, vol. 2021, Article ID 1526931, 9 pages, 2021.
- [19] A. Willfahrt, E. Steiner, J. Hötzel, and X. Crispin, "Printable acid-modified corn starch as non-toxic, disposable hydrogel-polymer electrolyte in supercapacitors," *Applied Physics A: Materials Science & Processing*, vol. 125, no. 7, pp. 1–10, 2019.
- [20] M. Alsaffar, G. Alshammari, A. Alshammari et al., "Detection of tuberculosis disease using image processing technique," *Mobile Information Systems*, vol. 2021, Article ID 7424836, 7 pages, 2021.
- [21] J. R. Gamage, A. K. M. DeSilva, D. Chantzis, and M. Antar, "Sustainable machining: process energy optimisation of wire electrodischarge machining of Inconel and titanium super-alloys," *Journal of Cleaner Production*, vol. 164, pp. 642–651, 2017.
- [22] A. Taneja, S. Rani, A. Alhudhaif, D. Koundal, and E. S. Gündüz, "An optimized scheme for energy efficient wireless communication via intelligent reflecting surfaces," *Expert Systems with Applications*, vol. 190, Article ID 116106, 2022.
- [23] M. B. Alazzam, A. A. Hamad, and A. S. AlGhamdi, "Dynamic mathematical models' system and synchronization," *Mathematical Problems in Engineering*, vol. 2021, Article ID 6842071, 7 pages, 2021.
- [24] A. Khadidos, A. Khadidos, O. M. Mirza, T. Hasanin, W. Enbeyle, and A. A. Hamad, "Evaluation of the risk of recurrence in patients with local advanced rectal tumours by different radiomic analysis approaches," *Applied Bionics and Biomechanics*, vol. 2021, Article ID 4520450, 9 pages, 2021.